

## INDUCTIVE SENSORS IN THICK FILM TECHNOLOGIES

**D. Marioli, E. Sardini and A. Taroni**

Department of Electronic Automation  
University of Brescia, Via Branze 38, 25123 Brescia Italy

*Abstract: The paper presents two thick film inductive sensors having different configuration: the first is a planar spiral while the second one consists of multi-layer spirals. The paper describes how the two sensors have been made, the materials used and their geometric configurations in order to optimize their metrological performances. The spatial distribution of the magnetic field generated by the two sensors has been simulated, while their impedance, the series-equivalent circuit parameters, as well as their sensitivity to temperature variation have been measured in the laboratory. Moreover the multi-layer sensor has been tested in the measurement of a metallic object profile. A processing electronics based on a synchronous demodulation technique extracts the inductance variation induced by the changing of the profile height. A preliminary test, cross calibrated with an optical system, shows an height resolution less than 10  $\mu\text{m}$  and a lateral resolution less than 2 mm.*

*Keywords: inductive sensor, thick film, profile measurement*

### 1 INTRODUCTION

In the field of proximity sensors, different commercial devices for industrial applications take advantage of the properties offered by the inductive transduction. Lately, literature reports papers [1,2] that describe inductive sensors of the planar type, realised with low-cost technologies and proposed for different applications such as coin recognition [3] and measurements of metallic object profile [4]. These sensors seem interesting to obtain measuring system having high performance at low cost: in our laboratory, two different types of inductive sensors have been developed. The first one is completely planar and its measuring performances suggest that it can be used as a proximity sensor while the second one is multi-layers and has been tested in profile measurement.

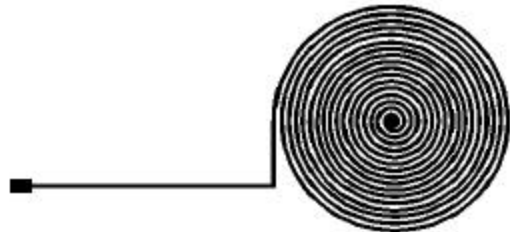


**Figure 1.** Planar inductive sensor

### 2 PLANAR SENSOR

#### 2.1 Description and Impedance characterization

The planar sensor consists of a track of conductive material (conductive paste C1075 Heraeus) deposited in a spiral form, as reported in figure 1, on an alumina substrate. The external diameter is 18 mm, the width and the thickness of the turns are respectively 200 and 20  $\mu\text{m}$ , while the distance between one spire and the following one is of 250  $\mu\text{m}$ . An isolating layer, 20  $\mu\text{m}$  thick covers the entire coil. The two sensor terminals are shown in the figure. The sensor impedance has been measured by using the impedance analyser HP 4194A and without the presence of any objects close to the sensor. The parameter of the equivalent series circuit consisting of a resistance ( $R_s$ ) and of an inductance ( $L_s$ ) has been evaluated to 2  $\mu\text{H}$  and 4.4  $\Omega$  at 150 kHz frequency. In order to increase the low inductance value, a ferromagnetic film has been attached on the back of the alumina substrate supporting the planar sensor. The thickness of this layer has been increased in various step from 0.1 up to 1 mm, increasing also the  $L_s$  value. The ferrite powder has been obtained by grinding a commercial ferrite and adding to the powder obtained additives in the measure of 25% of insulating paste IP9117 and 75% of powder. Anyway to obtain greater  $L_s$  value, it should be necessary to increase the ferromagnetic film thickness and it was not possible due to technology limits. For this reason, a thin

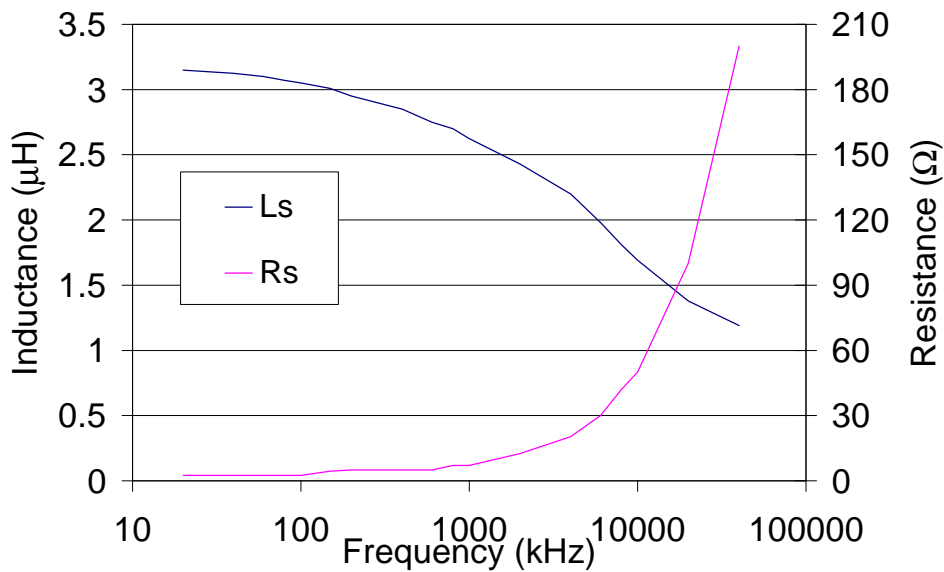


**Figure 2.** Equivalent series parameters of the planar sensor as a function of frequency

layer of mu-metal (having relative permeability  $\mu_r$  and thickness equal to 1000 and 25  $\mu\text{m}$  ) was attached to the back of the alumina substrate: figure 2 shows the  $L_s$  and  $R_s$  curves measured. Notice the absence of resonance (typical of the parasitic capacitance) up to 40 MHz  $L_s$  and  $R_s$  became 3,01  $\mu\text{H}$  and 4.38  $\Omega$  at 150 kHz.

## 2.2 Magnetic Field Simulation

To have an idea of the magnetic field distribution created by the sensor, a simulation program of static magnetic fields was used. (This cannot take into account the effects induced by the eddy-current). According to the simulation program, the magnetic field intensity in the radial component ( $B_r$ ) becomes marginal at a distance of about 200  $\mu\text{m}$  along the z axis, while the orthogonal component ( $B_z$ ) falls to 50% and to 90% of its maximum value at a distance from the centre, in the radial direction, of 2.5 and 5.5 mm respectively. A new simulation set was carried out on that planar sensor on which a mu-metal layer was added obtaining substantially the same relative spatial distribution of the magnetic field.

## 3 MULTI-LAYERED SENSOR

### 3.1 Description and Impedance characterisation

To confine the magnetic field in a spatial area smaller than the one of the preceding sensor, it is necessary to reduce the external diameter of the spiral. In order not to decrease the already low inductance value (which depends on the square of the number of the spires [5]), it would have been necessary to reduce the width of the conductive tracks, maintaining the number of the spires the same. The operation would have been feasible only by using a power laser, since the width of the preceding sensor tracks have already exploited the technology available as much as possible. An alternative solution consists in making a sensor with multi-layered, overlapping spires, as outlined in figure 3, where also the current direction rotates counter-clockwise in each spire. Simulations of the magnetic field of different geometry varying the number of layers and the number of spires have been carried out, for the purpose of confining B in a smaller spatial area and increasing the value of inductance. The sensor then consists of 10 overlapping layers, each one separated by an isolating layer. Each spiral consists of four turns and has an external diameter of 3,6 mm. The distance between each turn is 250  $\mu\text{m}$ , while the width and the track

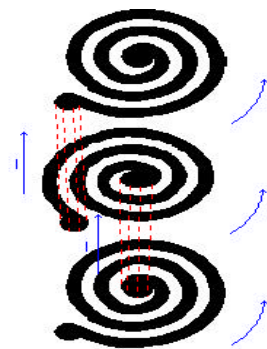


**Figure 3.** Multilayer sensor

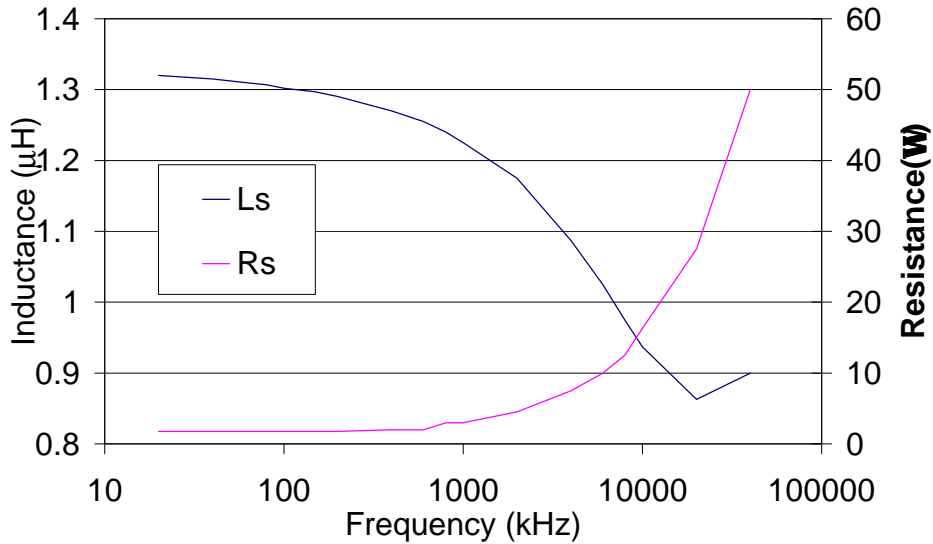


**Figure 4.** Equivalent series parameters of the multi-layer sensor as a function of frequency

thickness are respectively 250 and 20  $\mu\text{m}$ . Also in this case a mu-metal layer has been attached to the back of the alumina substrate. The curves of the equivalent series parameters  $L_s$  and  $R_s$  have been measured and are reported in figure 4. The  $L_s$  and  $R_s$  parameters are 1,30  $\mu\text{H}$  and 1,78  $\Omega$  at 150 kHz.

### 3.2 Magnetic field simulation

The simulation program of the magnetic fields gives the idea of the intensity and the direction of the magnetic field. While  $B_r$  is marginal at a 200  $\mu\text{m}$  distance in the perpendicular direction with respect to the substrate, component  $B_z$  of the magnetic field turns out to be confined in a narrower region. In fact, the  $B_z$  intensity decreases to 50% and 90% of its maximum value at a distance from the centre, in the radial direction, of 0,75 and 1,5 mm.

### 3.3 Working Frequency and temperature sensibility

The sensitivity to an orthogonal displacement of a target depends on the working frequency and on the target material being the distinction between ferromagnetic and diamagnetic the main important factor. For this reason, two square sheets 50  $\mu\text{m}$  thick and having 10 mm side has been moved from a starting position closed to the sensor to a distance of 200  $\mu\text{m}$  in the orthogonal direction to the sensor. The variations induced on  $L_s$  and  $R_s$  at different frequencies are reported in

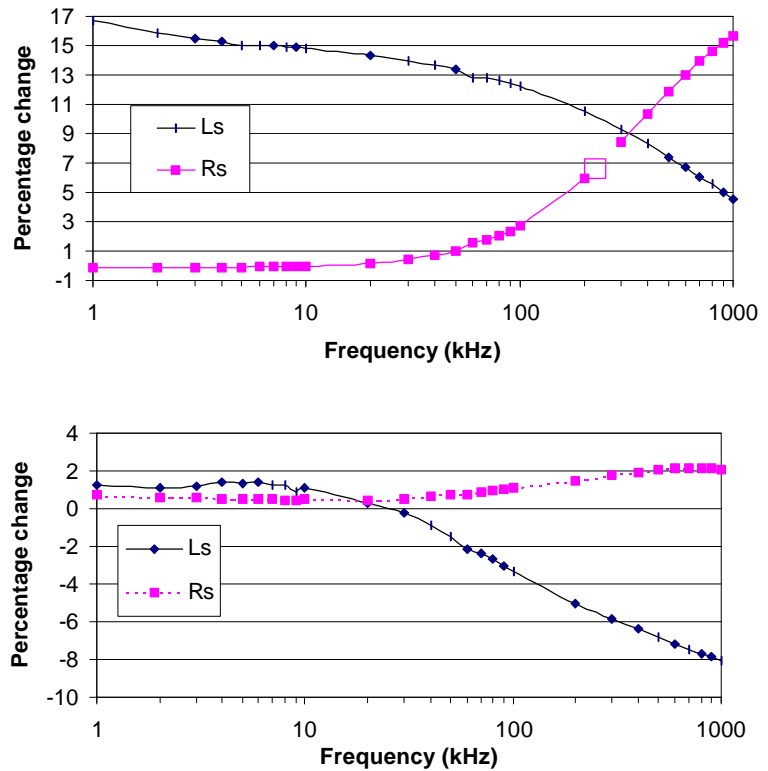
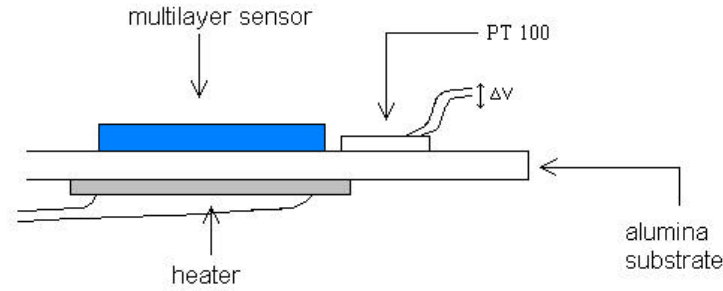
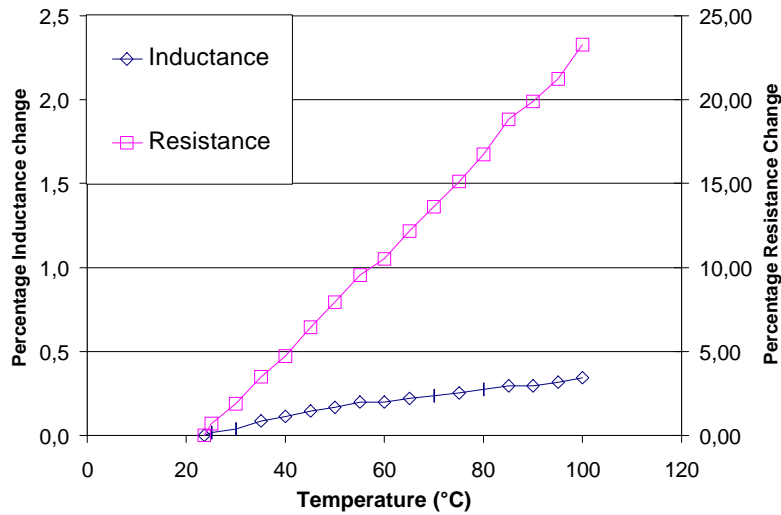


**Figure5.** Percentage change of  $R_s$  and  $L_s$  of a ferromagnetic material (up) and non-ferromagnetic material (down).



a)



b)

**Figure 6.** In a): set-up for the sensibility to temperature measurement, in b) inductance and resistance series equivalent parameters as functions of temperature.

figure 5. The first square is iron, ferromagnetic type, while the second is brass, a non-ferromagnetic material.

Because the objects whose profile should be determined, could be both ferromagnetic and diamagnetics and in order to use a fixed frequency value, a good compromise to have the higher sensitivity value as possible, is to select 150 kHz. This frequency let the use of low cost operational amplifier for the processing electronics.

To evaluate the measuring performance, a sensitivity curve of the equivalent series parameters  $L_s$  and  $R_s$  as a function of temperature has been obtained with the set-up shown in figure 6.a.. On the upper face of the alumina substrate there are the multilayer sensor and the temperature sensor (Pt100) while on the lower face there is the heater. The  $L_s$  and  $R_s$  curves, evaluated at 150 kHz, are shown as a function of temperature in figure 6.b: the inductance changes much less than the resistance, and is in the order of 50 ppm/°C.

### 3.4 Measurement circuit

Figure 7 shows a block scheme of the circuit used to process the signal coming from the sensor.  $V_s$  is a sinusoidal voltage at 150 kHz frequency that supplies two voltage to current converters generating each a  $I$  current of the same value but opposite in phase.  $V_1$  and  $V_2$ , the voltage generated by the  $I$  current on the sensor and the reference respectively, are summed, but being opposite in phase a difference of  $V_1$  and  $V_2$  is performed. The reference is a series of an inductor and a resistor of the same value  $L$  and  $R$  of the inductive sensor when any object is placed in front of it.

$\Delta L$  and  $\Delta R$  represent the variation induced by the presence of the target in front of the sensor.  $V_{diff}$ , the output voltage from the summing circuit, is equal to:

$$V_{diff} = \frac{R_2 k V_s}{R_1} (s \Delta L + \Delta R)$$

In the time domain, supposing  $V_s$  equal to  $\cos(\omega t)$ ,  $V_{diff}$  becomes:

$$V_{diff} = \frac{R_2 k}{R_1} [\Delta R \cos(\omega t) + \Delta L \sin(\omega t)]$$

$V_{diff}$  is then sent to the input of two multipliers. The first one, having as the other input the  $V_s$  signal, extracts with the aid of the low pass filter the  $V_{diff}$  cosine component. The second multiplier having, as input, a signal leading  $\pi/2$  with respect to  $V_s$  signal, gives the  $V_{diff}$  sine component, after the processing of the low pass filter. The cut-off frequencies of the two low pass filters are both located to 10 Hz.

### 3.5 Profile reconstruction

A metallic object, whose surface has two steps having heights of tens of  $\mu\text{m}$  has been used to test the sensor. The profile of this object has been previously determined by using an optical instrument having an accuracy of  $2 \mu\text{m}$ , a resolution of  $0.2 \mu\text{m}$ , and a movement step in the horizontal direction of  $50 \mu\text{m}$ . The measurements obtained are reported as continuous line in figure 8. As it can be seen the steps heights are  $50$  and  $30 \mu\text{m}$  approximately.

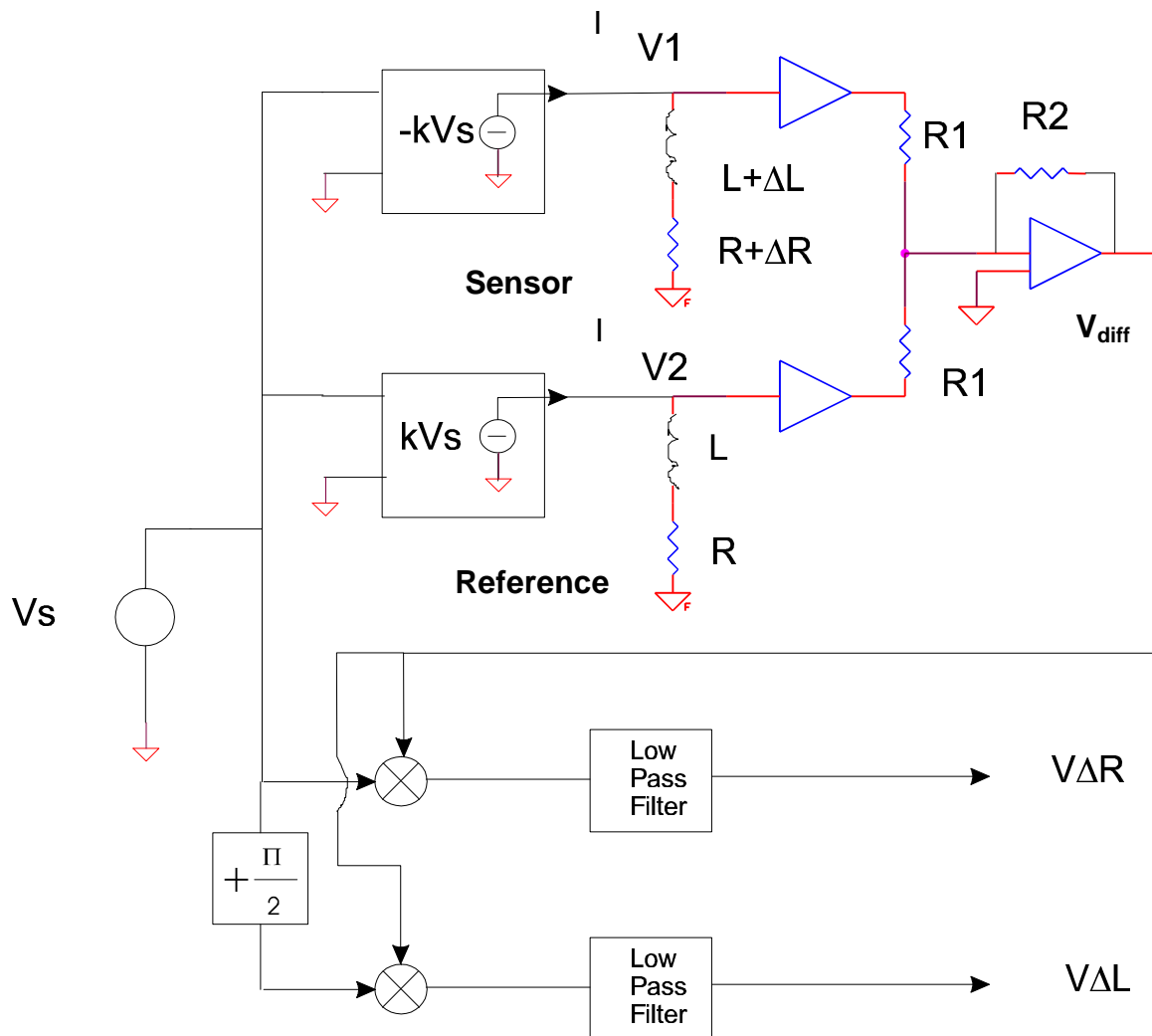
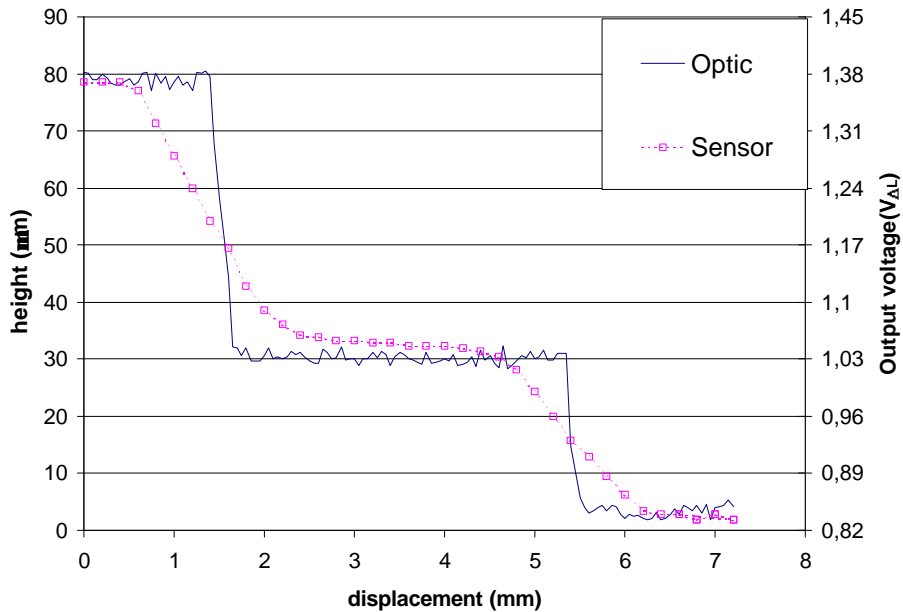


Figure 7. Block scheme of the electronic circuit



**Figure 8.** In continuous line, the profile of a metallic object as measured by an optical profilometer. The dot line represents the output voltage due to an inductance change as measured

The metallic object has been placed to a 300  $\mu\text{m}$  distance from the sensor and the measurements obtained, i.e.  $V_{\Delta L}$ , are reported as dot line in figure 8. The two curves agree quite well far away from the edges. In the closeness of the edge, the sensor lateral resolution is less than 2 mm, approximately what it has been predicted by the simulation.

Although having available two outputs, only the output voltage referred to inductance change has been reported due to the much less sensitivity to temperature variation according to the previous figure 6.b. Anyway also the shape of the  $\Delta R$  output voltage strictly looks like its  $\Delta L$  output voltage.

#### 4 CONCLUSIONS

Two different inductive sensors have been realised. The first is completely planar and the simulation show a lateral resolution of about 5 mm (50% of the maximum value of  $B$ ) while the second one, made of multi-layers, has a more contained lateral resolution of 1.5 mm. Due to their lateral resolution, the multi-layers sensor has been used in profile measurement application. The results obtained evidences a lateral resolution of 1.5 mm. and a height resolution of few  $\mu\text{m}$ .

#### REFERENCES

- [1] C. Bartoletti, R. Buonanni, L.G. Fantasia, R. Frulla, W. Gaggioli, G. Sacerdoti, The design of a proximity inductive sensor, in *Meas. Sci. Technol.*, **9** (1998) 1180-1190.
- [2] P.A. Passeraub, P.A. Besse, S. Hediger, Ch. de Raad, R.S. Popovic, High resolution miniaturized inductive proximity sensor: characterization and application for step-motor control, in: *Sensors and Actuators A* **68** (1998) 257-262
- [3] P.A. Passeraub, P.A. Besse, S. Hediger, Ch. de Raad, O. Dezuari, F. Quinet, R.S. Popovic, Metallic profile and coin imaging using an inductive proximity sensor microsystem, in: *Sensors and Actuators A* **66** (1998) 225-230 .
- [4] H. Fenniri, A. Moineau, G. Delaunay, Profile imagery using a flat eddy-current proximity sensor", in: *Sensors and Actuators A* **45** (1994) 183-190.
- [5] P.A. Passeraub, P.A. Besse, R.S. Popovic, Scaling down an inductive proximity sensor, *Sensors and Actuators A* **52** (1996) 114-118.

**AUTHORS:** Prof. Daniele MARIOLI, Prof. Andrea TARONI and Prof. Emilio Sardini, Department of Electronics for Automation, Faculty of Engineering, University of Brescia, Via Branze 38 - 25123 Brescia, Italy, Phone Int. +39-030-3715627, Fax Int. +39-030-380014, E-mail: sardini@ing.unibs.it